

Synchronisation of particle motion induced by mode coupling in a two-dimensional plasma crystal

L. Couëdel¹, C.-R. Du⁴, S. Zhdanov², V. Nosenko^{2,3},

A. Ivlev², H. Thomas^{2,3}, and G.E. Morfill²

¹ CNRS, AMU, Laboratoire PIIM, 13397 Marseille cedex 20, France.

² Max Planck Institute für extraterrestrische Physik, 85741 Garching b. München, Germany.

³Forschungsgruppe Komplexe Plasmen, Deutsches Zentrum für Luft und Raumfahrt, Oberpfaffenhofen, Germany.

⁴ College of Science, Donghua University, Shanghai 201620, People's Republic of China.

Abstract

The kinematics of dust particles during the early stage of mode-coupling induced melting in a two-dimensional plasma crystal is explored. The formation of the hybrid mode induces the partial synchronisation of the particle vibrations at the hybrid frequency. A rhythmic pattern of alternating in-phase and anti-phase oscillating chains of particles is observed. The spatial orientation of the synchronisation pattern correlates well with the directions of the maximal increment of the shear-free hybrid mode.

Introduction

Patterns are often observed in finite ensembles of interacting elements driven away from equilibrium and forced beyond a critical threshold [1]. Spontaneous emergence of synchronised signals and spontaneous symmetry breaking are typical behaviours in large populations of interacting units. A large system of weakly coupled nearly identical oscillators with a phase-dependent interaction is normally considered as a model to explore collective synchronisation. In two-dimensional plasma crystals, wake-mediated interactions between the particles result in the coupling of the crystal in-plane and out-of-plane modes into a hybrid mode of the lattice layer [2, 3, 4, 5]. A two-dimensional plasma crystal can be seen as an ensemble of coupled non-linear oscillators.

In this study, we show that the formation of the hybrid mode induces the partial synchronisation of the particle vibrations at the hybrid frequency. Alternating in-phase and anti-phase oscillating chains of particles are observed. The spatial orientation of the synchronisation pattern correlates well with the directions of the maximal increment of the shear-free hybrid mode.

Experiment

Mode coupling and plasma crystal melting were systematically investigated in experiments performed with a (modified) GEC chamber, in a capacitively coupled rf glow discharge at 13.56 MHz. The argon pressure was between 0.4 Pa and 1 Pa and the forward rf power was between 5 W and 20 W. A horizontal monolayer was formed by levitating melamine-formaldehyde particles ($9.19 \pm 0.14 \mu\text{m}$ diameter) in the plasma sheath above the lower rf electrode. The dust particle cloud was illuminated by two laser sheets: a vertical one and a horizontal one and imaged through a window at the top of the chamber by a camera at a speed of 250 frames per second. The horizontal coordinates x and y as well as velocity components v_x and v_y of individual particles were then extracted with sub-pixel resolution. An additional side-view camera was used to verify that our experiments were carried out with a single layer of particles. A detailed description of the experiment is given in Ref.[6].

Results

Tracking data obtained were used to compute the particle velocity fluctuation spectra. First the particle current components $V_s(\mathbf{k}, t) = \sum_{j=1}^N v_{s,j}(t) e^{-i\mathbf{k} \cdot \mathbf{s}_j(t)}$, were calculated in the s -direction at the time moment t , using a wave vector $\mathbf{k} = \{k_x, k_y\}$ located in the horizontal plane. Here, i is the imaginary unit, j is the particle index, $v_{s,j}(t)$ is the s -projection of the j -th particle velocity, $\mathbf{s}_j = \{x_j, y_j, z_j\}$ is its position, and N is the number of microparticles. x, y -axis were chosen as shown in Ref.[6]. A fast Fourier transform in time domain is then implemented to obtain the current fluctuation spectra. The structure factor of the crystal was also calculated from the particle positions $S(\mathbf{k}, t) = \frac{1}{N} \left| \sum_{j=1}^N e^{-i\mathbf{k} \cdot \mathbf{s}_j(t)} \right|^2$.

The 'hot spot' at the frequency $f_{hyb} = 16 \pm 1$ Hz, indicating emergence of the hybrid mode, is well pronounced in the longitudinal velocity fluctuation spectrum. As predicted by the linear isotropic theory [3, 5], it is the 'most unstable' direction.

The synchronised non-linear state of the crystal layer oscillations happened to be highly anisotropic; see Fig. 1 (left panel). Inside the first Brillouin zone, the hot spot located at $\theta = 60^\circ$ is about 9 times brighter than its 'counterpart' located at $\theta = -120^\circ$. The hot spots expected to be at $\theta = -60^\circ$ and 120° by symmetry have astonishingly disappeared. Therefore the energy spectrum of the synchronised hybrid mode oscillations is strongly intensity and angle modulated and the hexagonal symmetry of the crystal state is broken.

The displacements $r_j(t) = \sqrt{x_j^2(t) + y_j^2(t)}$ at hand were first filtered to remove the drift and to keep only the oscillatory parts, i.e., the "filtered" displacement $\tilde{r}_j(t)$ of the j th particle is defined as $\tilde{r}_j(t) = r_j(t) - \frac{1}{\Delta t} \int_{t-\frac{\Delta t}{2}}^{t+\frac{\Delta t}{2}} r_j(t') dt'$ where Δt , the interval of averaging, was chosen to be the same, $\Delta t = 0.5$ s, at all $j = 1 \dots N$. Finally the Hilbert transform was implemented to

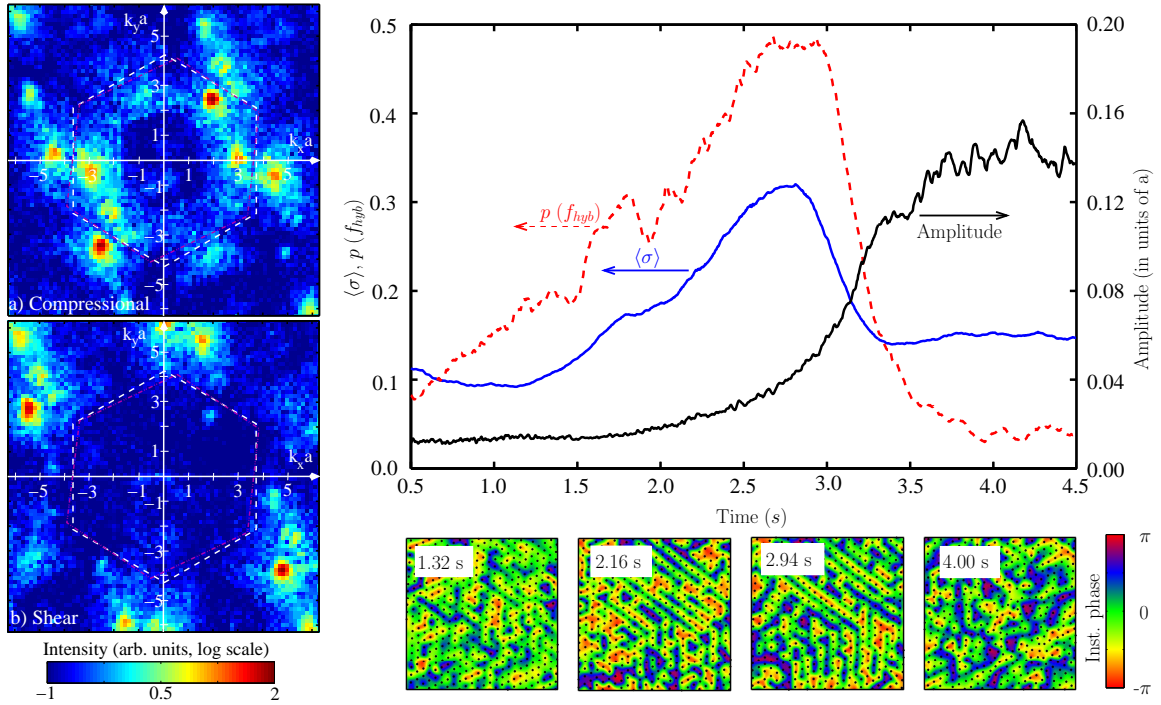


Figure 1: (Left) Spectrum of the particle velocity fluctuations in the $\{k_x, k_y\}$ -plane integrated over the frequency range $14 \text{ Hz} < f < 18 \text{ Hz}$. a) Compressional component. b) Shear component. White dashed lines: ideal first Brillouin zone. Dotted-dashed purple lines: real first Brillouin zone from time averaged structure factor. (Top-right) Evolution of the cumulative probability $p(f_{hyb})$ (red dashed curve) to find a particle with an instantaneous frequency in the band $14 \text{ Hz} < f < 18 \text{ Hz}$ around f_{hyb} , the mean synchronisation index $\langle \sigma \rangle$ (averaged over the particles, solid blue curve) and the averaged instantaneous amplitude of the particle oscillations (solid black curve). (Bottom-right) Consecutive snapshots indicating the instantaneous phase distribution for de-synchronised phase states ($t = 1.32$ s and $t = 4.00$ s), and during the synchronisation state ($t = 2.16$ s and $t = 2.94$ s). Black dots show the position of the particles.

obtain the analytic signals $r_{a_j}(t)$, their instantaneous phases, instantaneous frequency, and amplitudes. The instantaneous phase computed for each particle j was used to calculate the degree of synchronisation σ_j between the particle j with its closest neighbours; see Ref.[6].

The evolution of the cumulative probability $p(f_{hyb})$ to find the instantaneous frequency inside the frequency band 14-18 Hz around the hybrid resonance $f_{inst} \sim f_{hyb}$ is presented in Fig. 1 (top right). At start ($t < 0.5$ s), the frequency synchronisation probability is low. Then, as the mode coupling instability sets in, the probability gradually increases as more particles get locked at the hybrid frequency. Between $t = 2.5$ s and $t = 3$ s, a significant fraction of the particles oscillate at the hybrid frequency (partial frequency synchronisation state). When the crystalline suspension melts (at $t > 3$ s), the cumulative probability drops down stepwise indicating no frequency synchronisation (no mode coupling). The snapshots of the instantaneous phase variation are

presented in the bottom panels of Fig. 1 (bottom right). The phase locking proceeds as follows: (i) At $t < 1$ s, no recognisable synchronisation pattern. (ii) Starting from $t \simeq 1.3$ s, short rows of in-phase oscillating particles can be detected. (iii) With time passed, at $t = 2.16$ s, rows of the in-phase oscillating particles elongate as more particles become to be involved into synchronisation. Neighbouring rows of the synchronically oscillating particles are moving almost in anti-phase. (iv) Later on, at $t = 2.94$ s, two types of the phase alignment, one oblique (corresponding to the wave propagation angle $\theta \simeq 60^\circ$) and another almost vertical (corresponding to the wave propagation angle $\theta \simeq 0^\circ$), are seen (two equivalent directions, by symmetry, in the crystal). The synchronisation effect can also be well identified through the increase in the mean value of the synchronisation index $\langle \sigma \rangle$. (v) The degree of phase synchronisation is maximal when the probability to find the frequency locked in the vicinity of the hybrid resonance is also maximal. (vi) The pair correlation function $g(r)$ shows that the crystalline structure preserves for a long time. At $t > 3$ s, when the oscillations become too intense, the crystal melts, the synchronisation degree goes down and the particle oscillations de-synchronise.

Discussion and conclusion

It was shown that during the mode coupling induced melting, the formation of the unstable hybrid mode leads to the partial synchronisation of the particle motion in the direction of the main instability. It was evidenced by analysis of the instantaneous phase, instantaneous frequency and synchronisation index. The frequency and the phase synchronisation processes can be explained by the fact that only wave modes at the hybrid frequency have a positive growth rate while the other modes are well-attenuated by the damping.

This work was supported by the European Research Council under the European Union's Seventh Framework Programme (FP7/2007-2013) / ERC Grant agreement 267499, and by the French-German PHC PROCOPE program (Project 28444XH/55926142).

References

- [1] D.I.Goldman, M.D. Shattuck, S.J. Moon, *et al.*, Phys. Rev. Lett. **90**, 104302 (2003).
- [2] A. V. Ivlev and G. Morfill, Phys. Rev. E **63**, 016409 (2001).
- [3] S. K. Zhdanov, A. V. Ivlev, and G. E. Morfill, Phys. Plasmas **16**, 083706 (2009).
- [4] L. Couëdel, V. Nosenko, A. V. Ivlev, *et al.*, Phys. Rev. Lett. **104**, 195001 (2010).
- [5] L. Couëdel, S. K. Zhdanov, A. V. Ivlev, *et al.*, Phys. Plasmas **18**, 083707 (2011)
- [6] L. Couëdel, S. K. Zhdanov, V. Nosenko, *et al.*, Phys. Rev. E **89**, 053108 (2014)